2D Necklace Flower Constellations applied to Earth observation missions

D. Arnas[a,*], D. Casanova[b,c], E. Tresaco[b,c]

[a] *Massachusetts Institute of Technology, Cambridge, USA*
[b] *Centro Universitario de la Defensa, Zaragoza, Spain*
[c] *APEDIF-IUMA. Universidad de Zaragoza, Spain*

Abstract

This work focuses on the nominal design and later maintenance of satellite constellations based on the 2D Necklace Flower Constellations for their application in Earth observation missions. To that end, we introduce a generalization of the 2D Necklace Flower Constellations formulation to adapt the methodology to constellations whose satellites have different mission requirements, while still allowing to reduce the searching space in satellite constellation design. Moreover, this design is combined with its dual distribution in the Earth Centered Earth Fixed reference frame to obtain additional information about the dynamic of the system, including the sub-satellite point revisiting time, or the relative to Earth distribution. This is used to optimize the constellation in terms of maximum uniformity of the distribution with respect to the Earth. Finally, a detailed example of application of this design methodology is presented, where a constellation based on satellites with different mission requirements is considered.

Keywords: Satellite Constellation, Optimization, Mission Analysis, Perturbed dynamics, Orbit maintenance

*Corresponding author
Email address: arnas@mit.edu (D. Arnas)

1. Introduction

In the last decades, an increasing number of space missions are being designed based on the idea of cooperation between satellites. This has been seen extensively in telecommunication missions and global positioning systems. In general, such missions consist on satellites with identical (or very similar) payloads with the objective to provide either continuous or discontinuous coverage over given regions of the Earth surface. In order to study these systems, a large variety of satellite constellation designs have appeared. Examples of that include Walker Constellations [1], Streets of Coverage [2], Draim Constellations [3], Flower Constellations [4], or the kinematically regular satellite networks [5], but there are many others [6, 7, 8, 9, 10, 11, 12, 13, 14, 15]. Nevertheless, an increasing interest of combining the scientific data of different satellites have appeared in the last years with the objective of optimizing the use of the available resources in space, requiring, to that end, the coordination of the dynamic of different missions. One example of this kind of design is the A-Train [16] or the future plans for the Copernicus program [17]. However, the majority of the previous constellation designs assume that all the satellites in the constellation are identical, which limits their direct application to these systems. To overcome this limitation, Necklace Flower Constellations was introduced [18, 19, 20, 21].

Necklace Flower Constellations is a constellation design framework developed as a generalization of Flower Constellations [4, 24, 22, 23], and its later incarnation, the Lattice Flower Constellations [25, 26, 27]. The idea behind Necklace Flower Constellations is to generate a fictitious constellation containing all the possible satellite locations that are compatible with the mission requirements. This means that, in general, this fictitious constellation contains a larger number of satellites that the constellation sought. Therefore, a subset of these fictitious satellites is selected in such a way that the constellation maintains a chosen set of properties. The formulation of Necklace Flower Constellations has been applied for the 2D [28, 18], 3D [19], and 4D [21] Lattice Flower Constellations methodologies showing their possibilities in satellite constellation design and

their properties. However, no clear relation between mission requirements and the theory was presented, which limited its application to mission analysis.

In this work we focus on the design methodology of 2D Necklace Flower Constellations for different missions. Particularly, a complete example of application of this methodology for an Earth observation mission is presented, where we show the relation between mission requirements and the 2D Necklace Flower Constellation formulation. In this example, a constellation composed by very different satellites is shown, meaning that each satellite has very different mission requirements. This case of study introduces an additional complexity to the problem, being not all the satellites equivalent, which differs from other design methodologies such as Walker [29, 30] or Flower Constellations [31, 32]. Moreover, and in order to show a more in-depth study, we apply a formulation based on the Earth Centered - Earth Fixed (ECEF) frame of reference [33, 34, 35] to the same design and show the duality and benefits that the combined use of both formulations can provide.

Additionally, and due to the nature of this systems, it is also of interest to study the long term evolution of these systems under the effects of orbital perturbations. In that regard, other studies have dealt with the effects of orbital perturbations in satellite constellations, including Walker [36], Draim [37], Tundra [38], or the Galileo [39] constellations. For the more specific case of 2D Lattice Flower Constellations, a study on the effects of the oblateness of the Earth [40] (represented by the J_2 term of the Earth gravitational potential), and other orbital perturbations [41] was also studied. In this work, an example of control strategy is shown for 2D Necklace Flower Constellations applied to Earth observation missions to show that the design methodology proposed is feasible in terms of control and fuel budget, even in the cases where the constellation is comprised by satellites with very different mass properties.

This work is presented as follows. First, we introduce a summary of the methodologies of 2D Necklace Flower Constellations and the relative to Earth constellation formulation that we will use in this work. This summary includes the relation between both formulations, and a new generalization of 2D Necklace

Flower Constellations to account for non-uniformities in the distribution. Second, a mission concept is proposed for the application of these methodologies, including the selection of payloads and all the requirements that are considered in this study. Third, we include the definition of the nominal design of the constellation by means of the 2D Necklace Flower and the relative to Earth formulations. This allows to clearly show how to apply these design methodologies to particular mission requirements. Fourth, we define a control strategy for the mission and evaluate the orbital maneuvers required by each satellite of the constellation. With all these results, a simple but complete study of an Earth observation constellation mission is shown.

2. Constellation design methodology

The constellation design methodology presented in this work is based primarily on the 2D Necklace Flower Constellations, which is then complemented by a relative to Earth constellation definition in order to obtain additional information about the distribution. For that reason, a short summary of both methodologies is included in this section as a reference.

2.1. 2D Necklace Flower Constellations

2D Necklace Flower Constellations [18] (2D-NFC) is a constellation design methodology where all the satellites share their nominal values of semi-major axis (a), eccentricity (e), inclination (i) and argument of perigee (ω), while the mean anomaly (M) and right ascension of the ascending node (Ω) depend on each satellite of the constellation. 2D Necklace Flower Constellations has its foundation on the 2D Lattice Flower Constellation [25] (2D-LFC) methodology, which defines the following constellation distribution with respect to a reference satellite of the constellation:

$$\begin{pmatrix} L_\Omega & 0 \\ L_{M\Omega} & L_M \end{pmatrix} \begin{pmatrix} \Delta\Omega_{ij} \\ \Delta M_{ij} \end{pmatrix} = 2\pi \begin{pmatrix} i-1 \\ j-1 \end{pmatrix}, \tag{1}$$

being L_Ω the number of orbital planes of the constellation, L_M the number of satellites per orbit, $L_{M\Omega}$ the combination number (a parameter that allows to

shift the distribution between different orbital planes), $\Delta\Omega_{ij}$ and ΔM_{ij} represent the satellite distribution in the right ascension of the ascending node and the mean anomaly with respect to a reference satellite, and $i \in \{1, \ldots, L_\Omega\}$ and $j \in \{1, \ldots, L_M\}$ are the integer indexes that allow to define each satellite in the orbit i of the constellation and the position j of the orbit.

The 2D-LFC methodology generates uniform and symmetric configurations. However, provided a set of satellites, the number of possible different configurations is limited by the number of combinations between the distribution parameters [20], and thus, larger constellations are able to generate a larger number of different distributions. Therefore, in order to overcome this limitation and allow more flexibility in the design, the concept of Necklace was introduced [18].

The idea of Necklaces is to generate a fictitious constellation with a larger number of satellites that the constellation required, and then select a subset of those satellites following a given criteria. In that sense, the fictitious constellation is generated in such a way that all the fictitious satellites fulfill the mission requirements, while the real satellites are the subset that makes the constellation optimal for the mission considered.

The original 2D-NFC formulation [18] can be generalized to include a certain degree of non-uniformities that will be useful when dealing with constellations whose satellites have different mission requirement. In particular, it is possible to generate necklaces in the two distribution variables, Ω and M:

$$\begin{aligned} i &= \mathcal{G}_\Omega(i^*), \\ j &= \mathcal{G}_M(j^*) + P_{M\Omega}(i^*), \end{aligned} \tag{2}$$

where $\mathcal{G}_\Omega \subseteq \{1, \ldots, L_\Omega\}$ and $\mathcal{G}_M \subseteq \{1, \ldots, L_M\}$ are the necklaces in Ω and M respectively, and $i^* \in \{1, \ldots, N_\Omega\}$ and $j^* \in \{1, \ldots, N_M\}$ name each real satellite of the constellation. Note that using this formulation L_Ω and L_M define the number of available positions in each variable while N_Ω and N_M names the actual satellites of the constellation regarding their position in right ascension of the ascending node and mean anomaly. Finally, $P_{M\Omega} \in \{0, \ldots, Sym(\mathcal{G}_M)-1\}$ is a phasing parameter that allows to shift the configuration from one inertial

orbit with respect to the others, where $Sym(\mathcal{G}_M)$ is defined as the symmetry of the necklace $\mathcal{G}_M$, which represents the minimum number of rotations that a given necklace can perform without repeating the configuration, that is:

$$\mathcal{G}_M \equiv \mathcal{G}_M + Sym(\mathcal{G}_M), \tag{3}$$

where $\equiv$ identifies equivalent configurations. That way, the distribution of a 2D-NFC is defined by:

$$\begin{aligned} \Delta\Omega_{i^*j^*} &= \frac{2\pi}{L_\Omega}\left(\mathcal{G}_\Omega(i^*) - 1\right), \\ \Delta M_{i^*j^*} &= \frac{2\pi}{L_M}\Big((\mathcal{G}_M(j^*) - 1) + P_{M\Omega}(i^*) - \frac{L_{M\Omega}}{L_\Omega}\left(\mathcal{G}_\Omega(i^*) - 1\right)\Big). \end{aligned} \tag{4}$$

Note that this formulation differs slightly to the one presented in Ref. [18] to account for non-uniform distributions. This means that Eq. (4) represents a generalization of the 2D-NFC formulation.

Using Eq. (4), it is possible to obtain complete congruent configurations as the ones seen in previous works [18, 19, 21], that is, constellations distributions that are independent of the orbital planes selected as the reference. This kind of distributions are able to maintain the original properties of uniformity and symmetries of 2D Lattice Flower Constellations if some conditions are met. An in-depth study of these constellations can be seen in Ref. [18]. Following that work, the condition that the phasing parameter has to fulfill in order to obtain a congruent distribution is:

$$P_{M\Omega}(i^*) = S_{M\Omega}(\mathcal{G}_\Omega(i^*) - 1), \tag{5}$$

being $S_{M\Omega} \in \{1, \ldots, Sym(\mathcal{G}_M)\}$ the shifting parameter, an integer constant for the distribution that must fulfill the following relation to generate a congruent distribution:

$$Sym(\mathcal{G}_M) \mid S_{M\Omega}L_\Omega - L_{M\Omega}, \tag{6}$$

which reads $Sym(\mathcal{G}_M)$ divides $S_{M\Omega}L_\Omega - L_{M\Omega}$, and where the previous expression is a Diophantine equation used to obtain the solution of $S_{M\Omega}$.

2.1.1. Repeating ground-track property

In addition to the previous formulation, it is possible to impose the repeating space-track property [35] (if required). This is done by applying the compatibility condition to the distribution:

$$N_p \Delta\Omega_{ij} + N_d \Delta M_{ij} = 0 \mod (2\pi) \tag{7}$$

where N_p is the number of orbital revolutions and N_d is the number of days to ground-track repetition respectively. This means that, there are two conditions that 2D-NFC must fulfill to obtain a repeating ground track constellation [35]. First, $L_M | N_d$ and $\gcd(N_d/L_M, L_\Omega) = 1$ to impose that satellites in the same orbit belong to the same ground-track, and second:

$$N_d L_{M\Omega} + A L_\Omega L_M = N_p L_M, \quad \text{where} \quad A \in \mathbb{Z}, \tag{8}$$

to select the combination number that locates satellites from different orbital planes in the same ground-track. A more in-depth study of the implications of these parameters and examples of application can be found in Ref. [18].

2.2. Relative to Earth constellation formulation

In this work we will make use of the formulation provided by Ref. [33]. This formulation allows to define satellite constellations directly in the ECEF frame of reference using as distribution variables the along-track and cross-track distances between satellites. The idea behind this methodology is to define a set of reference space-tracks that are shared by subsets of satellites of the constellation. This means that the values of the nominal semi-major axis, inclination, eccentricity and argument of perigee for all the satellites of the constellation are common, as in the case of 2D-NFC. Additionally, and when dealing with completely uniform distributions, this formulation becomes:

$$\begin{aligned} \Delta\Omega_{kq} &= -2\pi N_d \frac{q-1}{N_{st}}, \\ \Delta M_{kq} &= 2\pi \frac{N_p}{N_d} \frac{k-1}{N_t \gcd(N_p, N_t)} + 2\pi N_p \frac{q-1}{N_{st}}, \end{aligned} \tag{9}$$

where $\Delta\Omega_{kq}$ and ΔM_{kq} are the right ascension of the ascending node and mean anomaly of each satellite with respect to a reference satellite of the constellation; N_{st} is the number of satellites in each ground-track, N_t is the number of different ground-tracks of the constellation, and $q \in \{1, \ldots, N_{st}\}$ and $k \in \{1, \ldots, N_t\}$ are the distribution variables that name and locate each satellite in the track k of the constellation and the position q of each ground-track.

2.3. Relation between both formulations

It is possible to relate both formulations when dealing with constellations whose satellites are located in the same repeating ground-track [35]. In those cases $N_t = k = 1$, and Eq. (9) leads to [33]:

$$\begin{aligned} \Delta\Omega_{kq} &= -2\pi N_d \frac{(q-1)}{L_\Omega L_M} \mod (2\pi), \\ \Delta M_{kq} &= 2\pi N_p \frac{(q-1)}{L_\Omega L_M} \mod (2\pi), \end{aligned} \tag{10}$$

where $N_{st} = L_\Omega L_M$ is the number of fictitious satellites of the constellation. Then, we can relate the distribution in ΔM with the one defined in a 2D-LFC (see Eq. (1)), obtaining:

$$2\pi \left(\frac{j-1}{L_M} - \frac{L_{M\Omega}(i-1)}{L_\Omega L_M} \right) = 2\pi N_p \frac{(q-1)}{L_\Omega L_M} \mod (2\pi), \tag{11}$$

and after some equation manipulation in modular arithmetic, the following relation is obtained:

$$N_p(q-1) + B\,(L_\Omega L_M) = (j-1)L_\Omega - (i-1)L_{M\Omega}, \tag{12}$$

or in the case of 2D-NFC:

$$N_p(q-1) + B\,(L_\Omega L_M) = \Big[(\mathcal{G}_M - 1 + P_{M\Omega})L_\Omega - (\mathcal{G}_\Omega - 1)L_{M\Omega}\Big], \tag{13}$$

where B is an unknown integer number, and L_Ω, L_M and $L_{M\Omega}$ fulfill the conditions presented before to obtain a repeating ground-track configuration. Equation (13) is a Diophantine equation in $(q-1)$ and B that defines the complete transformation between 2D-NFC and this relative to Earth formulation. This

means that Eq. (13) is able to relate the distribution in the inertial frame of reference (where the 2D-LFC and 2D-NFC are defined) with the ECEF frame of reference (where the formulation from Eq. (9) is defined), allowing for instance, to compute the revisiting time between satellites, or the sequence of passing of all the satellites of the constellation over a given area. In that regard, it is important to note that all the distributions generated using this formulation are uniform, and thus, the relative positions between satellites are known in both reference systems.

In the next sections we deal with a mission concept and its related mission requirements. Under these conditions, we propose a constellation design based on the methodology presented, and study its dynamic under orbital perturbations. This example of application is selected to show clearly how to apply the previous methodologies using real mission requirements. In that sense, the satellite distribution has been selected in such a way that the resultant constellation is able to fulfill all the mission requirements while keeping the process followed as clear as possible.

3. Mission concept

In this work, we propose a constellation for coordinated Earth observation based on 6 satellites whose mission is land remote sensing based on both optical and radar instruments. In particular, each satellite of the constellation will carry a single instrument, meaning that a coordination between satellites is required in order to be able to combine the scientific data from different payloads. To that end, instruments shall be able to study the same Earth regions under a similar geometry, that is, the data obtained from all the satellites of the constellation should be from the same regions of the Earth and taken under the most similar conditions, including orientation of cameras and instruments, and Earth-Sun-Instrument geometry. This condition allows to combine the scientific data of different satellites and reduce the revisiting time of the mission. Moreover, an additional requirement of the mission is that the constellation shall be able to

cover the majority of Earth's surface in the least number of days. This implies that the revisiting time of the constellation must be minimal, not only regarding each individual satellite, but also from the constellation as a whole, and from the perspective of the different payloads.

This kind of mission concept has already been applied to several missions, and its use is expected to increase in the future due to the number of possibilities that it provides in new missions, and also because it allows to optimize the satellites available. An example of this kind of mission concept is the coordination of Sentinel-3A with Sentinel-3B (or the future Sentinel-3C/D) [17] and other smaller missions such as FLEX [42].

For this example, the constellation considered is based on the instruments carried by the Earth observation missions Landsat 7 [43], OCO-2 [44] and CloudSat [16], where each two satellites of the constellation have the same or equivalent payloads. This introduces in the problem studied three different families of instruments, which will have some interesting results during the design of the constellation. Moreover, this study focuses on a constellation made of only 6 satellites to show how the methodology applies in a varied set of mission requirements while keeping the number of satellites, and thus the complexity of the system, low enough to make the manuscript as clear as possible.

Landsat program is the oldest family of satellites whose mission is the acquisition of satellite imagery of the Earth. The program focuses on monitoring the landmass of the Earth, providing high spatial resolution images both in the visible and the infrared specters of light. The first satellite of the family, the Earth Resources Technology Satellite (later renamed Landsat 1), was launched in 1972 providing nearly three years of operation to the mission. Other satellites of the family followed the program: Landsat 2 (1975−1982), Landsat 3 (1978−1983), Landsat 4 (1982−1993), Landsat 5 (1984−2013), Landsat 6 (1993−1993), Landsat 7 (1999−) and Landsat 8 (2013−). In addition, Landsat 9 is expected to be launched in 2020. In this work we focus on Landsat 7 instrument, the Enhanced Thematic Mapper Plus (ETM+), and the requirements that this instrument imposes to the mission. The ETM+ is an imaging radiometer with eight spectral

bands that ranges from the visible blue to the far infrared.

CloudSat mission is part of the Earth Observing System (EOS) Afternoon Constellation, also known as the A-train, a tandem formation actually based on six satellites: Aqua, Aura, CALIPSO, CloudSat, GCOM-W1 and OCO-2. The aim of CloudSat is the study of clouds with the objective of characterizing the role they play in regulating the Earth's climate. The satellite was launched in 2006 and its primary payload is the Cloud Profiling Radar (CPR), a 94-GHz radar with 500-m vertical resolution.

The Orbiting Carbon Observatory (OCO) is a satellite mission that was intended to provide observations on the atmospheric carbon dioxide from a near polar orbit. However, the first satellite of the series, OCO, was lost in a launch failure in 2009. Later, in 2014, OCO-2 was successfully launched to substitute OCO. One interesting property of OCO-2 is that the satellite maintains a loose formation with the A-train, providing complementary scientific data to the mentioned constellation. The primary payload of OCO-2 consists of three high resolution grating spectrometers.

4. Mission requirements

The mission considered is based on six satellites and two kinds of payloads: two different spectrometers (from Landsat 7 and OCO-2) and a radar (from CloudSat). In addition, each two satellites of the constellation will contain the same or an equivalent payload. This introduces a set of distinct mission requirements for each satellite of the constellation that they must fulfill in order to provide scientific data for the mission.

Now, we present the mission requirements for each satellite, showing the constraints that each instrument introduces in the problem as well as the physical properties of the satellites that originally carried these payloads. In that respect, and in order to show the requirements in a clearer manner, we have separated each satellite class in a different point.

4.1. Landsat 7 class satellites (ETM+)

For this mission, we assume that the two Landsat 7 class satellites will be the primary spacecrafts of the mission, since they are the heaviest satellites that we are considering. This means that, during the design, we will focus on the requirements of these two satellites, being the requirements of the other satellites additional constraints that will be applied to this first set of requirements.

The ETM+ is an instrument with a field of view of $\pm 7.5°$ and a swath of 185 km, which requires to fly at a nominal of altitude 705 km $\pm$ 5 km at the equator. Moreover, this payload requires to perform periodically 3 different kind of calibrations that affects the selection of the orbit [45, 46, 47]:

- Ground Look Calibration (GLC): this calibration consists on the observation of given areas of the Earth surface, that, due to their properties of homogeneity and stability over the course of the year, allow to perform measure comparisons. It is carried out each 2 to 6 months during the normal operation of the satellite. Examples of this reference regions are Railroad Valley Playa (38.5° N, 115.7° W) and White Sands (32.9° N, 106.4° W).

- Full Aperture Solar Calibration (FASC): this calibration is performed each 4 to 6 weeks during the normal operation of the satellite and consists on the observation of the Sun using a set of mirrors in the instrument while the satellite lays in the frontier between day and night and flies over the polar circle region.

- Partial Aperture Solar Calibration (PASC): this calibration is performed once per day and lasts for two minutes. It consists on the measurement of the radiation of the Sun while the satellite has just exited an eclipse and its sub-satellite point is still in a night region.

Additionally, there are two more requirements that the ETM+ must fulfill. First, the local time at the ascending node must be between 09:45 and 10:15. Second, and in order to maintain the observation geometric properties, the

orbit inclination of the satellite must be in the range of $\pm 0.15^\circ$ from the sun-synchronous inclination.

On the other hand, the size and weight of the satellite also influences the dynamic of the spacecraft. In that respect, we select Landsat 7 as the reference for this class of satellites. Landsat 7 has a mass of 1982 kg, its height is 4 m and presents 2.7 m of diameter [48, 175-179]. These dimensions will be used in order to evaluate the effect of the atmospheric drag in the satellite.

4.2. OCO-2 class satellites (grating spectrometer)

The instrument of OCO-2 (a payload consisting of three grating spectrometers) requires a sun-synchronous orbit with a local time at the ascending node between 13:18 and 13:33, a nominal altitude over the equator of around 705 km, and an inclination control of $\pm 0.1^\circ$ with respect to its sun-synchronous inclination. Furthermore, OCO-2, the reference satellite for this class of satellites, has a weight of 530 kg, a longitude of 2.3 m and 1.4 m of diameter [48, 199-203].

4.3. CloudSat class satellites (CPR)

The CPR instrument does not introduce more requirements to the mission (since it share many of the previous constraints presented for Landsat 7 and OCO-2). In that respect, CPR requires also a sun-synchronous orbit with an altitude of around 705 km over the equator. In addition, the reference satellite used in this work, CloudSat, has a mass of 999 kg and the following dimensions: 2.3 m $\times$ 2.3 m $\times$ 2.8 m [48, 125-128].

4.4. Global requirements of the constellation

In addition to the requirements imposed by each instrument of the mission, the constellation satellites are required to maintain the same ground-track. This is done primarily for three reasons. First, the constellation is required to maintain the geometry of the observations over the target regions over time. This allows not only to compare the data of different passes, but also to combine the scientific data from different satellites. Second, this condition allows to ease the

communications with the ground segment providing a periodic dynamic. Finally, the perturbation produced by the Earth gravitational potential affects all the constellation satellites in the same manner since they follow the same trajectory in the ECEF reference system [35]. This allows to maintain the relative position of satellites more easily.

In that regard, we assume that all the constellation satellites have a ground-track control both in plane and in inclination. The boundaries of this control are the same for all the satellites of the constellation in order to maintain the structure of the system as a constellation. In particular, we select the most restrictive requirements from the mission instruments to define a dead band of 1.5 km (in each direction) and a range of inclinations of ± 0.01 from the sun-synchronous inclination.

Moreover, and in order to improve the response of the constellation as a system, the constellation proposed will be designed is such a way that the revisiting time for all the regions covered by the constellation will be the smallest possible with the considered requirements. That way, we will be able to show an application case of 2D-NFC in optimization problems.

5. Nominal design of the constellation

Based on the mission requirements presented, it is possible to define the nominal design of the constellation. In order to do that, we first define the reference orbit for the constellation, that is, an orbit that fulfills the mission requirements and that will be used to generate the constellation reference trajectory in the ECEF frame of reference. Then, the design of the constellation is performed using the 2D-NFC.

5.1. Nominal reference orbit

Based on the requirements of repetition from the calibration of the ETM+, as well as for convenience of design related to data handling and performance of the mission, we select a repeating ground-track sun-synchronous frozen orbit.

Moreover, since all the satellites of the constellation require to observe the same regions of the Earth under similar geometries, we impose that all satellites of the constellation share the same ground-track. This means that the nominal values of the eccentricity, inclination, argument of perigee and semi-major axis of all the satellites of the constellation will be the same [33].

Table 1: Repetition parameters of some compatible orbits.

$\mathbf{N_p}$	233	262	277	291	306	335
$\mathbf{N_d}$	16	18	19	20	21	23
$\mathbf{N_p}$	364	379	393	408	422	437
$\mathbf{N_d}$	25	26	27	28	29	30

However, although the payloads of the constellation are required to fly at an altitude of around 705 km, we do not know exactly the semi-major axis of the orbit nor its eccentricity or inclination. In order to obtain them, we impose the requirements of repeating ground-track orbit, sun-synchrony, and that the swath of the ETM+ is able to cover all the Earth at the end of the repeating cycle. By applying these conditions, we can obtain a series of compatible orbits [49, 862-895]. A summary of the orbits that have the lowest repetition time and fulfill the mission requirements can be seen in Table 1.

Table 2: Orbital parameters of the nominal orbit of the constellation.

Nominal a	7077.722 km
Nominal i	98.186°
Nominal e	0.001043
Nominal ω	90.000°
Ω and M	Dependent on the date and satellite

Table 1 shows that the orbit with best repetition time is the one with $N_p = 233$ and $N_d = 16$. Thus, we select it as the nominal orbit for the constellation. This means that each satellite of the constellation will repeat its ground-track in 233 orbit revolutions or 16 days. Moreover, and since we want the orbit to be as

stable as possible, we impose that the satellites of the constellation present the frozen orbit property [49, 885-888]. With these conditions, the nominal values of the semi-major axis, the eccentricity, the inclination, and the argument of perigee of the orbits are obtained [50]. Table 2 presents a summary of the nominal orbital parameters of the constellation.

5.2. Nominal constellation distribution

Once the nominal orbit of the constellation is defined, we can now focus on the constellation distribution. The first step for this is to determine the size of the fictitious constellation. This fictitious constellation defines the complete set of possible positions where a satellite of the constellation can be located to fulfill all mission requirements. This means that if a satellite is located in one of these positions, it is guaranteed that it will fulfill the mission requirements considered for this study.

From the mission requirements of Landsat 7 and OCO-2 (the satellites that have an optical sensor), we know that the local time in the ascending node for their orbits must be from 09:45 to 10:15 and from 13:18 to 13:33 respectively. The local time is in fact providing the information of the angular distance that must exist between the orbital planes of both satellites. Particularly, this condition can be rewritten as $\Delta\Omega = [45.75^\circ, 57.0^\circ]$, from which an intermediate value of $\Delta\Omega = 51.43^\circ$ is selected as the nominal for the constellation distribution to be able to absorb the effects of orbital perturbations. In fact, this value is also chosen since it is the seventh part of a complete rotation ($360^\circ/7 \approx 51.43^\circ$), a fact that will greatly simplify the representations shown in this section while still fulfilling the mission requirements. Thus, a uniform fictitious constellation with 7 orbital planes is defined ($L_\Omega = 7$), and since the number of satellites that share instrument is two, we can derive that $N_\Omega = 3$, that is, satellites with similar instrument must be in the same orbital plane to fulfill their specific missions.

5.2.1. Generation of available positions

The next step is to determine the number of available positions that can be defined in each orbit in such a way that they are in the same ground-track. From the expression in $\Delta\Omega_{kq}$ of Eq. (10), if we impose that all the satellites belong to the same inertial orbit:

$$0 = -2\pi N_d \frac{(q-1)}{L_\Omega L_M} \mod (2\pi), \tag{14}$$

we can derive that the maximum number of available positions in each inertial orbit is equal to N_d (which corresponds to the nodes of the orbit). This means that the fictitious constellation that is compatible with the ground-track of the problem has $L_M = N_d = 16$ available positions in each orbit, where only two positions will be occupied by satellites of the constellation, that is, the number of real satellites per orbit is $N_M = 2$.

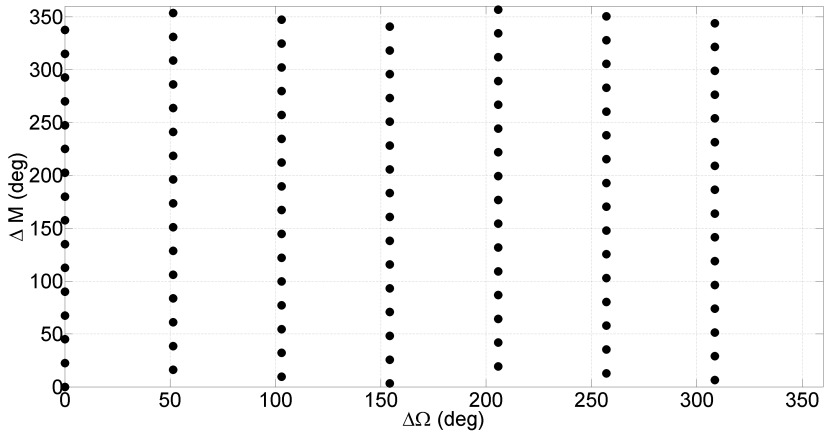

Figure 1: Representation of the fictitious constellation in the (Ω, M)-space.

Being L_Ω and L_M already known, only the combination number $L_{M\Omega}$ is left to be defined. Its value can be obtained using Eq. (8):

$$16 \cdot L_{M\Omega} + A \cdot 7 \cdot 16 = 233 \cdot 16, \tag{15}$$

where the combination number that allows the fictitious constellation to be distributed in only one ground-track is $L_{M\Omega} = 2$. Figure 1 shows the distribution

of the fictitious constellation in the (Ω, M)-space. It is important to note that the position of the reference satellite of the orbit will depend on the date, since orbits and satellites are rotating during the dynamic of the system.

5.2.2. Necklace selection

The objective now is to select the necklaces $\mathcal{G}_\Omega$ and $\mathcal{G}_M$ that will define the orbital planes selected, and the distribution of satellites in each orbital plane respectively. In that sense, these necklaces will be studied independently.

First of all, we define an orbital plane of reference. Since Landsat 7 class satellites are considered the primary spacecrafts of the mission, we select their orbital plane as the reference for the constellation. Then, from the mission requirements, we know that Landsat 7 and OCO-2 class satellites must be in two different planes at an angle of $51.43°$, which represent two consecutive planes of the fictitious constellation. On the other hand, we locate the orbital plane of CloudSat class satellites at the same angular distance but on the opposite direction. That way, the necklace to select must be $\mathcal{G}_\Omega = \{1, 2, 7\}$, where $\mathcal{G}_\Omega(1) = 1$ corresponds to Landsat 7 class satellites, $\mathcal{G}_\Omega(2) = 2$ relates to OCO-2 class satellites, and $\mathcal{G}_\Omega(3) = 7$ represents CloudSat class satellites.

Second, the necklace in the mean anomaly $\mathcal{G}_M$ must be selected. This necklace represents the distribution of satellites that share the same orbital plane or, in other words, the satellites that share the same payload. Since we are looking for the distribution with the smallest revisiting time in each payload, the along track distance between both must be maximum in order to optimize the revisiting time for any point in the Earth surface. That way, instead of having a revisiting time of 16 days for each instrument, the time will be reduced to half. Thus, satellites that share the same orbital plane must be phased 56 positions in the relative trajectory (from the total of $L_M L_\Omega = 112$ available positions), or in other words (see Eq. (10)):

$$\Delta M = 2\pi N_p \frac{56}{112} \mod (2\pi) = \pi. \tag{16}$$

This means that from the total of 16 available positions in each orbital plane, we

must select the pair of positions that are located at 180^o. This is represented by the necklace $\mathcal{G}_M = \{1, 9\}$ (both satellites are separated 8 positions from a total of 16 available positions), where $\mathcal{G}_M(1) = 1$ is the first satellite of each class and $\mathcal{G}_M(2) = 9$ is the second satellite of each class. Note that $Sym(\mathcal{G}_M) = 8$ due to the fact that:

$$\mathcal{G}_M + Sym(\mathcal{G}_M) \mod (L_M) = \mathcal{G}_M \longrightarrow \{1, 9\} + 8 \mod (16) = \{1, 9\}. \quad (17)$$

5.3. Phasing and revisiting time

Once the fictitious constellation and the necklaces are defined, it is time to study which is the optimal phasing combination between orbital planes that allows to obtain the minimum revisiting time for the constellation while fulfilling the mission requirements. In that regard, we will consider a worst-case scenario where the revisiting time is computed for any point in the ground-track and with no field of view. This means that we will focus in the revisiting times of the subsatellite points for any location along the ground-track of the constellation. This calculation is performed using the relations between 2D-NFC and the relative to Earth constellation formulation derived previously.

The period of repetition of the constellation dynamic in the ECEF frame of reference T_c is given by:

$$T_c = N_d \frac{2\pi}{\omega_\oplus - \dot{\Omega}}, \quad (18)$$

being $\dot{\Omega}$ the secular value on the variation of the right ascension of the ascending node, which, for this mission, corresponds also with the sun-synchronous secular drift of Ω. This means that, for a uniform distribution (as the ones studied in this work), two consecutive available positions in the constellation are separated an along track time distance equal to $T_c/(L_\Omega L_M)$. Therefore, it is possible to define the along track time distribution of the constellation with respect to a reference satellite through [34]:

$$t_q = \frac{(q-1)}{L_\Omega L_M} T_c, \quad (19)$$

where $q \in \{1, \ldots, L_\Omega L_M\}$ names each of the available positions of the fictitious constellation. Then, using Eq. (13), we can relate the distribution provided by

Table 3: Along track distribution of the constellation.

Phasing		Landsat 7 class		OCO-2 class		CloudSat class		Max.
OCO-2	Cloudsat	$\mathcal{G}_\Omega(1)$		$\mathcal{G}_\Omega(2)$		$\mathcal{G}_\Omega(3)$		Rev.
$\mathcal{G}_\Omega(2)$	$\mathcal{G}_\Omega(3)$	$\mathcal{G}_M(1)$	$\mathcal{G}_M(2)$	$\mathcal{G}_M(1)$	$\mathcal{G}_M(2)$	$\mathcal{G}_M(1)$	$\mathcal{G}_M(2)$	Time
$P_{M\Omega}(2)$	$P_{M\Omega}(3)$	q						(hours)
0	0	1	57	63	7	37	93	102.86
0	1	1	57	63	7	100	44	126.86
0	2	1	57	63	7	51	107	150.86
0	3	1	57	63	7	2	58	171.43
0	4	1	57	63	7	65	9	164.57
0	5	1	57	63	7	16	72	140.57
0	6	1	57	63	7	79	23	116.57
0	7	1	57	63	7	30	86	92.57
1	0	1	57	14	70	37	93	78.86
1	1	1	57	14	70	100	44	102.86
1	2	1	57	14	70	51	107	126.86
1	3	1	57	14	70	2	58	147.43
1	4	1	57	14	70	65	9	147.43
1	5	1	57	14	70	16	72	140.57
1	6	1	57	14	70	79	23	116.57
1	7	1	57	14	70	30	86	92.57
2	**0**	**1**	**57**	**77**	**21**	**37**	**93**	**68.57**
2	1	1	57	77	21	100	44	78.86
2	2	1	57	77	21	51	107	102.86
2	3	1	57	77	21	2	58	123.43
2	4	1	57	77	21	65	9	123.43
2	5	1	57	77	21	16	72	123.43
2	6	1	57	77	21	79	23	116.57
2	7	1	57	77	21	30	86	92.57
3	0	1	57	28	84	37	93	92.57
3	1	1	57	28	84	100	44	92.57
3	2	1	57	28	84	51	107	92.57
3	3	1	57	28	84	2	58	99.43
3	4	1	57	28	84	65	9	99.43
3	5	1	57	28	84	16	72	99.43
3	6	1	57	28	84	79	23	99.43
3	7	1	57	28	84	30	86	92.57
4	0	1	57	91	35	37	93	116.57
4	1	1	57	91	35	100	44	116.57
4	2	1	57	91	35	51	107	116.57
4	3	1	57	91	35	2	58	113.14
4	4	1	57	91	35	65	9	89.14
4	5	1	57	91	35	16	72	75.43
4	6	1	57	91	35	79	23	75.43
4	7	1	57	91	35	30	86	99.43
5	0	1	57	42	98	37	93	123.43
5	1	1	57	42	98	100	44	140.57
5	2	1	57	42	98	51	107	140.57
5	3	1	57	42	98	2	58	137.14
5	4	1	57	42	98	65	9	113.14
5	5	1	57	42	98	16	72	89.14
5	6	1	57	42	98	79	23	75.43
5	7	1	57	42	98	30	86	99.43
6	0	1	57	105	49	37	93	123.43
6	1	1	57	105	49	100	44	147.43
6	2	1	57	105	49	51	107	164.57
6	3	1	57	105	49	2	58	161.14
6	4	1	57	105	49	65	9	137.14
6	5	1	57	105	49	16	72	113.14
6	6	1	57	105	49	79	23	89.14
6	7	1	57	105	49	30	86	99.43
7	0	1	57	56	112	37	93	123.43
7	1	1	57	56	112	100	44	147.43
7	2	1	57	56	112	51	107	171.43
7	3	1	57	56	112	2	58	185.14
7	4	1	57	56	112	65	9	161.14
7	5	1	57	56	112	16	72	137.14
7	6	1	57	56	112	79	23	113.14
7	7	1	57	56	112	30	86	99.43

the 2D-NFC formulation with the one defined by Eq. (19). By following this procedure, it is possible to compute analytically the revisiting time between subsatellite points.

Moreover, we know that the phasing parameter for each orbital plane is bounded by $P_{M\Omega} \in \{0, \ldots, Sym(\mathcal{G}_M) - 1\}$, and thus, there is a limited number of possible configurations that must be studied. First, the orbital plane containing Landsat 7 satellites is selected as the reference of the constellation, so, this plane can be considered as having no phasing, that is, $P_{M\Omega}(1) = 0$. Therefore, under the mission requirements considered in this study, there are $Sym^2(\mathcal{G}_M) = 64$ possibilities of design. Table 3 shows all these possible configurations. In that regard, each constellation distribution is defined based on the phasing parameters $P_{M\Omega}(2)$ and $P_{M\Omega}(3)$. Table 3 contains the relative positions of the satellites with respect to their ground-track (q), as well as the maximum revisiting time between two satellites during the whole dynamic of the constellation.

5.3.1. Optimal configuration

From the results obtained in Table 3, it can be derived that the optimal solution with respect to the revisiting time is the one defined by the phasing parameters $P_{M\Omega}(2) = 2$ and $P_{M\Omega}(3) = 0$. The orbital parameters of this optimal constellation can be seen in Table 4. As mentioned in previous subsections, we select one of the Landsat 7 satellites as the reference spacecraft to define the constellation. Moreover, this distribution can be also represented in the (Ω, M)-space [25]. Such representation is shown in Figure 2, where the available positions from the fictitious constellation are shown as empty circumferences, while the real satellites of the constellation are represented by filled circles. As it can be seen, the solution presents a symmetry with respect to the orbital plane of reference that is different to the symmetries that can be generated with the original 2D-NFC formulation [18]. This shows that the generalized formulation introduced in Eq. (4) provides very interesting solutions for Earth observation missions that cannot be obtained with the original 2D-NFCs.

Table 4: Distribution of the constellation.

	Landsat 7 class $\mathcal{G}_\Omega(1)$		OCO-2 class $\mathcal{G}_\Omega(2)$		CloudSat class $\mathcal{G}_\Omega(3)$	
	$\mathcal{G}_M(1)$	$\mathcal{G}_M(2)$	$\mathcal{G}_M(1)$	$\mathcal{G}_M(2)$	$\mathcal{G}_M(1)$	$\mathcal{G}_M(2)$
$\Delta\Omega$	0.00°	0.00°	51.43°	51.43°	308.57°	308.57°
ΔM	0.00°	180.00°	38.57°	218.57°	321.43°	141.43°

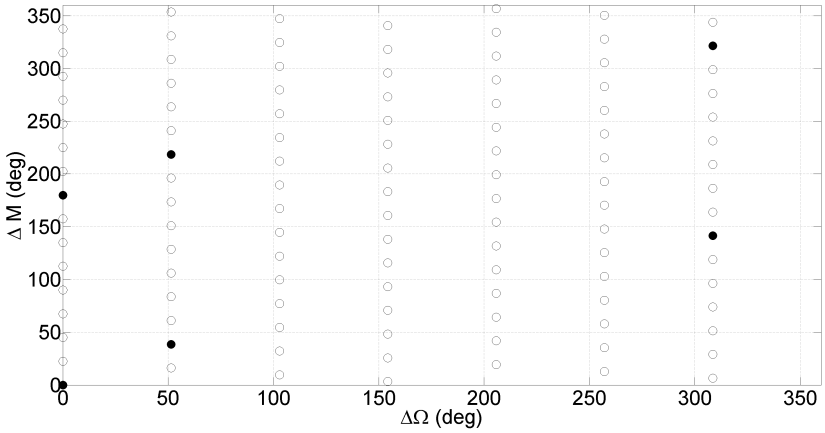

Figure 2: Representation of the real constellation in the (Ω, M)-space.

Figure 4 shows the inertial distribution of the constellation from the isometric and polar perspectives. On the other hand, Fig. 4 shows the relative to Earth representation of the constellation and its ground-track at a given instant.

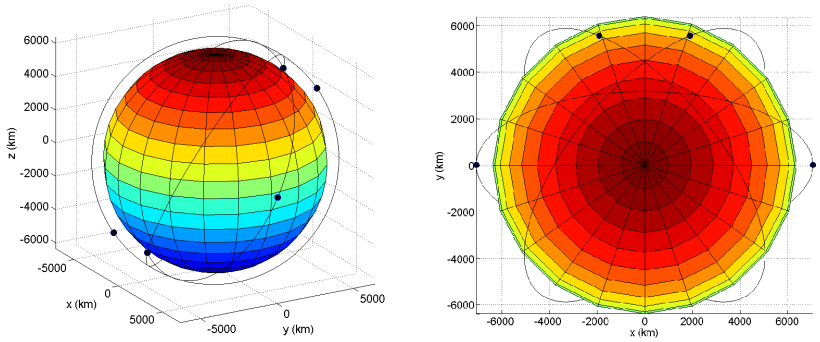

Figure 3: Inertial constellation distribution in isometric (left) and polar (right) perspectives.

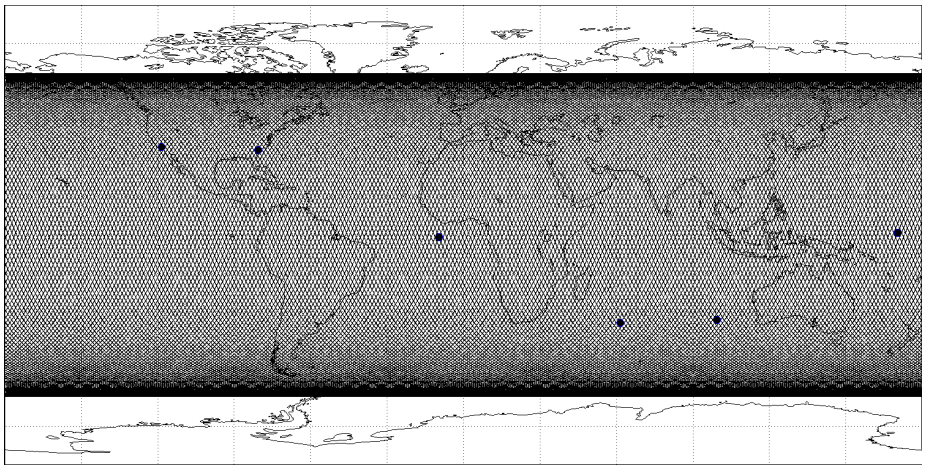

Figure 4: Relative to Earth and ground-track representation of the constellation.

6. Control strategy and station keeping

This defined nominal distribution can be maintained without any orbital maneuver under the effects of the J_2 perturbation [51, 52, 50]. However, if more terms of the Earth gravitational potential are considered, a numerical algorithm is required to define the nominal orbit such as the one in Vallado [49, 873] or Wagner [53]. That way, it is possible to maintain a frozen orbit, like the orbits considered, nearly indefinitely under these perturbations, being the maneuvers required negligible when compared to other orbital perturbations. Note also that under orbital perturbations, satellites of the same class have a slightly different inertial orbit due to the drift that orbital planes experiment during the time that it takes to fly from one satellite to its class companion [33, 35]. This result comes from the condition imposed in the sharing of the constellation ground-tracks.

In addition to the Earth gravitational potential, we consider in this study the atmospheric drag, the Sun and Moon as third bodies and the solar radiation pressure. In that respect, and due to the nature of the problem, we will separate their effects in in plane and out of plane maneuvers, which are more related to

the actual control of the satellites.

For this mission, we propose a control box strategy for the constellation [17]. This means that each satellite will have a defined boundary in which it is maintained. From the mission requirements, we have to impose a control in inclination of $\pm 0.01^{\circ}$ with respect to the sun-synchronous inclination and a dead band of ± 1.5 km, which corresponds approximately to the maximum deviation that the control in inclination produces in the ground-track of the orbits. This control box is applied to all the satellites of the constellation in order to maintain the formation over time.

On the other hand, and since the orbit and ground-track is being maintained, it is also of interest to know the variation that satellites experiment in their along-track distribution during the dynamic of the system. Thus, and as a result of the control strategy proposed, the along-track distances between satellites and their nominal positions will vary in a box of ± 3.225 s. This shows that even if the maneuvers of each satellite are unrelated, the configuration of the constellation is maintained. The following sections deal with the in plane and out of plane maneuvers required to maintain this constellation.

6.1. In plane maneuvers

In plane maneuvers have two objectives. The first one aims to counter the decay of the semi-major axis of the orbit due to the atmospheric drag, while its second objective consists on the maintenance of the ground-track of the orbit inside its defined dead band. These two effects are produced primarily by the atmospheric drag and the Sun and Moon as third bodies.

In this section we show the results for frequency between in plane maneuvers and impulse required for every satellite of the constellation. As it will be seen, these values depend on the physical properties of each satellite and the date in which the computation is considered. In that respect, we have selected the values of the real Landsat 7, OCO-2 and CloudSat as references for this study. A summary of their properties is provided in Section 4. All the in plane maneuvers are assumed to be performed when the satellites are in eclipse in order to not

disturb the normal acquisition of data. Table 5 presents a summary of the Δv required for each satellite to maintain the proposed configuration for 11 years.

Table 5: In plane Δv required for a 11 years mission for maximum, mean and minimum solar activity (SA).

	B_C	Δv (m/s)		
	(kg/m^2)	Max SA	Mean SA	Min SA
Landsat 7	157.2	7.03	1.60	0.54
OCO-2	156.4	12.50	2.79	0.80
CloudSat	85.8	4.78	1.41	0.64

In addition to the expected correction due to the orbital perturbations, a given number of collision avoidance maneuvers per year must be taken into account when defining the fuel budget. However, in most cases those maneuvers require to increase the semi-major axis of the orbit, and thus, do not produce an increase in the requirements of fuel for the mission (since this fuel is being used to improve the maintenance of the ground-track at the same time). For this reason, we do not treat these cases in this study.

The results presented in this section were computed using the NRLMSISE-00 model [54] for the atmospheric density and tabulated data from the European Cooperation for Space Standardization (ECSS) [55, 45-54] for the flux generated in a solar cycle. Moreover, we consider a constant density during each day. All the computations performed correspond to a complete solar cycle beginning on January of 2020. Note that if information about the mission for other dates not presented in here is required, these results can be extrapolated to other dates due to the eleven years periodicity that this model predicts for the solar cycle.

It is also important to note that the results presented in this section greatly depend on the ballistic coefficient of the satellites, the local time in their ascending nodes, and the solar flux. In that respect, the values of the solar flux (and thus, the atmospheric density) are a prediction of the future solar activity based on past solar cycles. On the other hand, the drag coefficients of the satel-

lites are an estimation based on past missions. This means that the calculation presented in this section has a high uncertainty due to these factors. However, these results present a baseline of the strategy and the order of magnitude of the maneuvers expected during the mission of these satellites.

6.1.1. Maneuver frequency

Figure 5 shows the maneuver frequency of the constellation satellites for an 11-year solar cycle and under the assumption of mean solar activity. As it can be seen, OCO-2 class satellites require to perform their in plane maneuvers more frequently than the other satellites. This is produced by the bigger ballistic coefficient of OCO-2 class satellites and the orientation of their orbit with respect to the Sun.

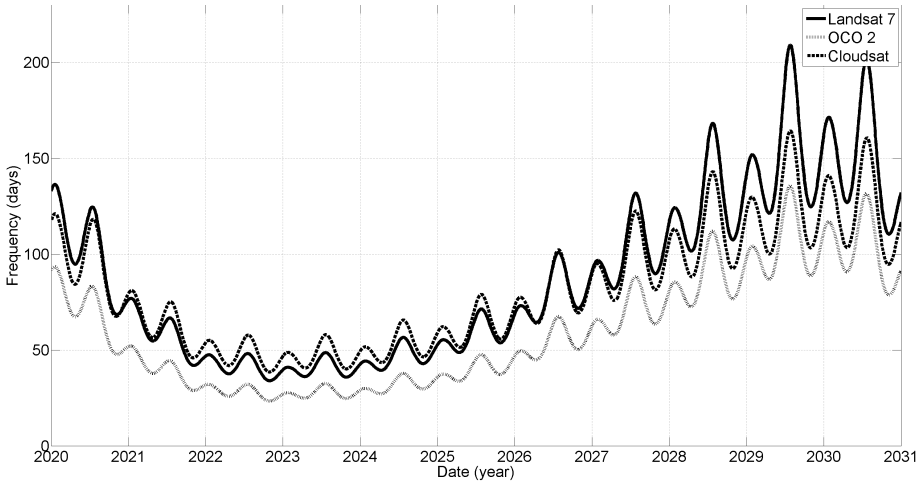

Figure 5: Maneuver frequency under mean solar activity

6.1.2. Impulse per maneuver

Moreover, it is possible to compute the impulse per maneuver required to maintain the nominal constellation configuration. Figure 6 shows the evolution of the impulse required per maneuver during a complete solar cycle of 11 years. As it can be seen from the figure, OCO-2 class satellites require a larger impulse per maneuver compared with the other satellites of the constellation.

As mention before, this is produced by their larger ballistic coefficient and the orientation of their orbits.

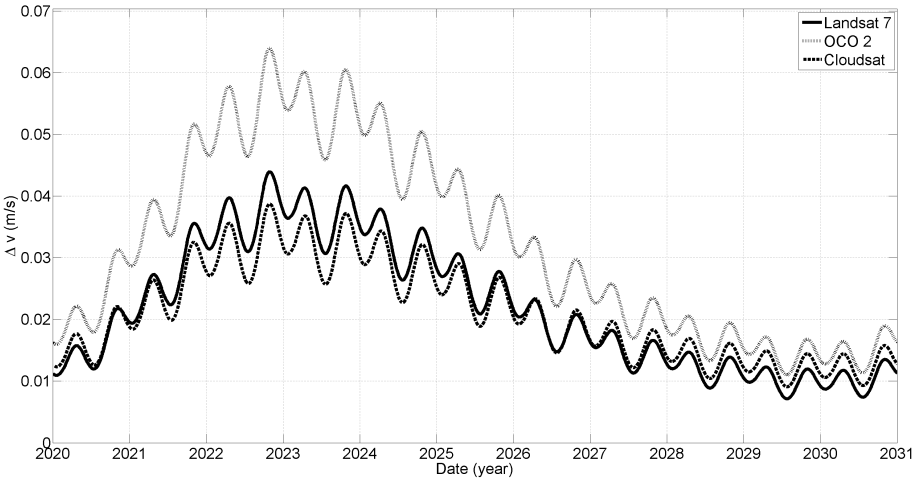

Figure 6: Impulse required per maneuver under mean solar activity

6.2. Out of plane maneuvers

Out of plane maneuvers aim to ensure the sun-synchrony of the orbit, the mean local solar time, and the maintenance of the ground-track of the constellation. The deviation produced in the inclination of the orbits is provoked primarily by the Sun and Moon as disturbing third bodies and the solar radiation pressure. In this section we present the results of the evolution of the inclination of the orbits under perturbations, and the out of plane maneuvers required to maintain the satellites in their defined control boxes.

For this study, we take into account the following perturbations: the Earth gravitational potential up to 4th order terms (including tesseral terms), the Sun and Moon as disturbing third bodies, the solar radiation pressure and the atmospheric drag (using the same model as in the in plane maneuvers). In addition, we assume that the out of plane maneuvers are performed once satellites reach their mission boundaries. This means that all the out of plane maneuvers will be based in a change of inclination of 0.02°, which leads to an impulse of

$\Delta v = 2.61957 m/s$ for each maneuver. Another important thing to notice is that out of plane maneuvers will modify the along track distribution of the constellation and thus, we must expect additional in plane maneuvers following each out of plane maneuver. Since these additional maneuvers are very dependent of the impulsive errors, we do not treat them in this study.

6.2.1. Landsat 7 class satellites

Figure 7 shows the evolution of Landsat 7 class satellites in the orbit inclination through one year of propagation. From this figure and the numerical data obtained, we can derive that for the boundary in the inclination considered, that is, $\pm 0.01°$, an out of plane maneuver should be planed for each Landsat 7 class satellite each 200 days of mission.

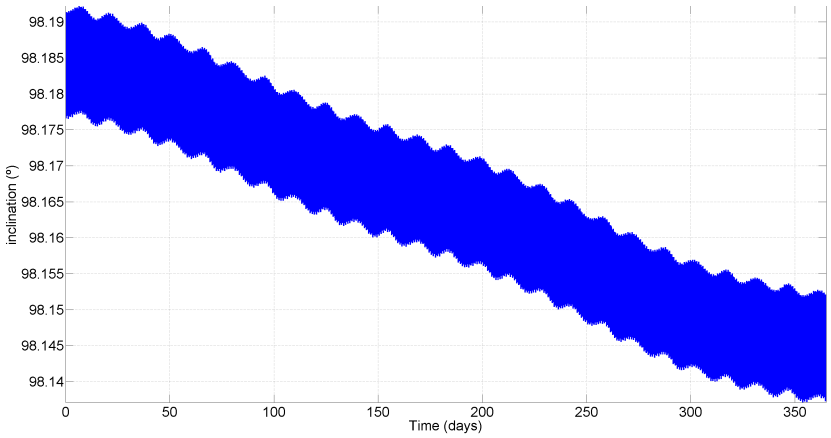

Figure 7: Inclination evolution of Landsat 7 class satellites.

6.2.2. OCO-2 class satellites

Figure 8 presents the evolution of the inclination for one year of propagation of the OCO-2 class satellites. From the figure and the numerical data produced during the propagation, we conclude that this class of satellites will require an out of plane maneuver each 260 days in order to fulfill the inclination mission requirements.

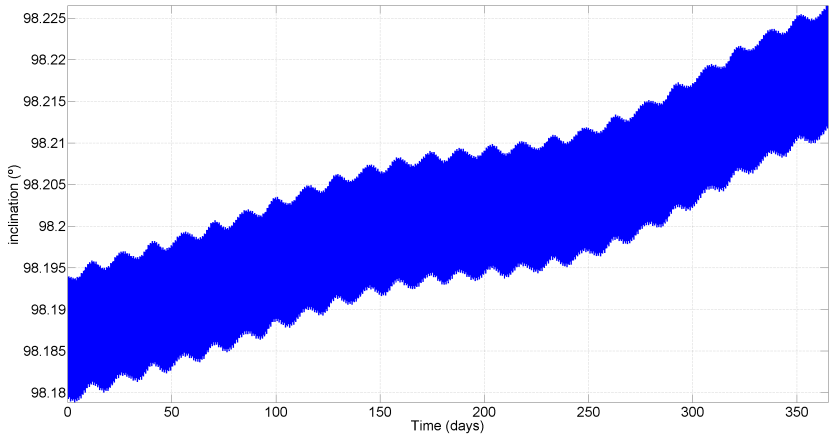

Figure 8: Inclination evolution of OCO-2 class satellites.

Additionally, it is important to note that the secular variation of the inclination experienced by OCO-2 class satellites is positive, compared to the Landsat 7 and CloudSat (presented later) class satellites which is negative. This effect is produced by the different orientation of the orbit of OCO-2 class satellites with respect to the Sun. In particular, OCO-2 class satellites orbit is the only one with a local solar time in the ascending node greater than the 12:00 hours, more precisely 13:26, which produces this important change in the evolution of the inclination. This differential variation in the inclination does not produce a large impact in the example presented, however, in high density orbits, for instance when dealing with megaconstellations, this could potentially generate an increase in satellite conjunctions due to the sensibility that the minimum distances between satellites has with respect to small changes in the inclination of the orbits [56].

6.2.3. CloudSat class satellites

Figure 9 shows the osculating evolution of the inclination for CloudSat class satellites for one year of propagation. However, in this case, after a year of propagation, the satellites are not able to reach the boundaries of the control box. In fact, the computation was continued, in order to obtain a frequency

between out of plane maneuvers. By doing so, we conclude that an out of plane maneuver is required each 600 days of mission.

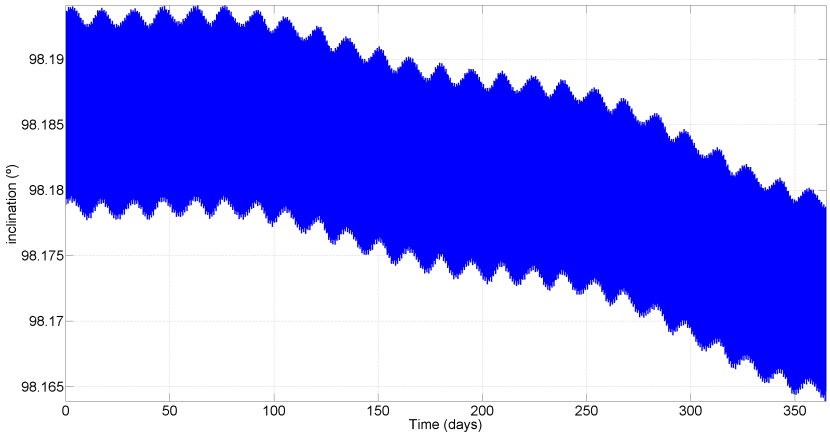

Figure 9: Inclination evolution of CloudSat class satellites.

Furthermore, comparing Landsat 7 class satellites inclination evolution with the one of CloudSat, we can see how CloudSat class satellites require a lesser number of out of plane maneuvers for the same time period. This is produced by the gyroscopic effect in the orbit, affecting more intensively to satellites near the 12:00 - 24:00 local solar time at the ascending node. In that respect, the reader should remember that there are two sets of equilibrium points in the inclination. The first one corresponds to the 06:00 - 18:00 orbits which are also know as dusk and dawn orbits (stable configuration); while the second set is comprised by the 12:00 - 24:00 orbits which are unstable.

7. Conclusions

This work focuses on the use of the 2D Necklace Flower Constellation methodology to design satellite constellations subject to a set of mission requirements. In that sense, we consider constellations whose satellites can have very different payloads, and study how these requirements translate into satellite constellation design parameters using a generalization of the 2D Necklace Flower Constellations formulation. In that sense, a complete example of application is presented,

where we select an Earth observation constellation consisting of 6 satellites having each two of them the same instrument. In particular, this work uses the payloads of Landsat 7, OCO-2 and CloudSat missions as the reference instruments to define the mission requirements for the constellation design considered.

Under the mission requirements studied, this work presents a feasible solution for this mission based on a combined design between the formulations of 2D Necklace Flower Constellations and a relative to Earth satellite constellation definition. This allows to have a direct control in the design process of the satellite distribution both in the inertial frame of reference and the ECEF frame of reference. To be more precise, this design process starts with the definition of a reference orbit for the constellation based on the mission requirements. Then, using the 2D Necklace Flower Constellations and a relative to Earth constellation formulation, we define the available positions of a fictitious constellation where all satellites fulfill the mission requirements. That way, it is possible to significantly reduce the searching space for the optimization of the system. Note that these available positions are the unique orbit locations that fulfill all mission requirements, and thus, they limit the number of possible satellite distributions at our disposal. After that, all the configuration possibilities are studied in terms of revisiting time, finding the optimal constellation under the conditions considered.

Additionally, a study on the effects of orbital perturbations in the constellation is included. More precisely, the Earth gravitational potential, the atmospheric drag, the Sun and Moon as third bodies and the solar radiation pressure are taken into account in this study. Thus, and in order to maintain the constellation within its mission requirements, a control box strategy is proposed where each satellite is controlled individually. From this study it is easy to derive that each satellite of the constellation is affected in a very different manner. This is due to two main circumstances. First, each satellite has a different mass properties, which implies differences in their ballistic coefficients. This difference is especially relevant when dealing with the atmospheric drag and the solar radiation pressure. Second, satellites are positioned in different inertial orbits. This

leads to a different dynamic under the effects of the Sun and Moon as third bodies. Moreover, having different inertial orbits also modifies the effects of the atmospheric drag and the solar radiation pressure since the local time at the ascending node of each satellite is different. Nevertheless, we show that using a control box strategy, 2D Necklace Flower constellations are able to fulfill the mission requirements of the constellation and maintain their structure with a low amount of fuel even when considering very different satellite mass properties and mission requirements for each spacecraft of the constellation.

It is important to note that all the methodologies presented in this work can be adapted to other missions without farther modification. In that sense, if more specific mission requirements have to be considered, additional constraints will be required to be imposed in the constellation design. Nevertheless, both formulations used in this work allow enough flexibility to adapt them to the most common mission requirements, while still being able to reduce the searching space for the optimization process.

Finally, this work shows a first study on how 2D Necklace Flower and a relative to Earth formulation can be combined in satellite constellation design to perform a dual definition of constellations, the first one from the inertial frame of reference, and the second one from the ECEF frame of reference. This allows to benefit from the properties of both methodologies, while also obtaining a more detailed information on the dynamic of the constellation from these reference systems. An example of this kind of application is the determination of the sequence of satellites from the Earth perspective.

Funding Sources

The work of David Arnas, Daniel Casanova, and Eva Tresaco was supported by the Spanish Ministry of Economy and Competitiveness, Project no. ESP2017–87113–R (AEI/FEDER, UE); and by the Aragon Government and European Social Fund (group E24_17R).

References

[1] Walker, J. G., *Satellite Constellations*, Journal of the British Interplanetary Society, Vol. 37, 1984, pp. 559-572. ISSN 0007-084X.

[2] Luders, R., *Satellite networks for continuous zonal coverage*, ARS Journal, Vol. 31, No. 2, 1961, pp. 179-184. doi: 10.2514/8.5422.

[3] Draim, J. E., *A common-period four-satellite continuous global coverage constellation*, Journal of Guidance, Control, and Dynamics, Vol. 10, No. 5, 1987, pp. 492-499. ISSN 0731-5090.

[4] Mortari, D., Wilkins, M. P. and Bruccoleri, C., *The Flower Constellations*, Journal of the Astronautical Sciences, American Astronautical Society, Vol. 52, No. 1-2, 2004, pp.107-127. ISBN: 978-0-87703-189-5.

[5] Mozhaev, G.V., *The problem of continuous Earth coverage and the Kinematically regular satellite networks*, Cosmic Research, Vol. 11, 1973, pp. 755.

[6] Ulybyshev, Y., *Satellite constellation design for complex coverage*, Journal of Spacecraft and Rockets, Vol. 45, No. 4, 2008, pp. 843-849. doi: 10.2514/1.35369.

[7] Lo, M. W., *Satellite-Constellation Design*, Computing in Science & Engineering, Vol. 1, No. 1, 1999, pp. 58-67. doi: 10.2514/1.35369.

[8] Beste, D.C., *Design of satellites constellations for optimal continuous coverage*, IEEE Transactions on Aerospace and Electronic Systems, No. 3, 1978, pp. 466-473. doi: 10.1109/TAES.1978.308608.

[9] Ballard, A.H., *Rossete constellations of Earth satellites*, IEEE Transactions on Aerospace and Electronic Systems, No. 5, Sept 1980, pp. 656-673. doi: 10.1109/TAES.1980.308932.

[10] Dufour, F., *Coverage optimization of elliptical satellite constellations with an extended satellite triplet method*, 54th International Astronautical

Congress of the International Astronautical Federation, the International Academy of Astronautics, and the International Institute of Space Law, International Astronautical Congress (IAF), A-3, 2003. doi: 10.2514/6.IAC-03-A.3.02.

[11] Rider, L., *Optimized polar orbit constellations for redundant earth coverage*, Journal of the Astronautical Sciences, Vol. 33, 1985, pp. 147-161. doi: 10.2514/6.IAC-03-A.3.02.

[12] Wook, S., Kronig, L.G., Ivanov, A.B., and Weck, O.L., *Satellite constellation design algorithm for remote sensing of diurnal cycles phenomena*, Advances in Space Research, Vol. 62, 2018, pp. 2529-2550. doi: 10.1016/j.asr.2018.07.012.

[13] Palmerini, G.B., *Hybrid configurations for satellite constellations*, in: Mission Design & Implementation of Satellite Constellations. Springer, Dordrecht, Netherlands, 1988, pp. 81-89. doi: 10.1007/978-94-011-5088-0_7.

[14] Ortore, E., Cinelli, M., and Circi, C., *A ground track-based approach to design satellite constellations*, Aerospace Science and Technology, Vol. 69, 2017, pp. 458-464. doi: 10.1016/j.ast.2017.07.006.

[15] Sarno, S., Graziano, M. D.,, and D'Errico, M., *Polar constellations design for discontinuous coverage*, Acta Astronautica, Vol. 127, 2016, pp. 367-374. doi: 10.1016/j.actaastro.2016.06.001 .

[16] Stephens, G. L., Vane, D. G., Boain, R. J., Mace, G. G., Sassen, K., Wang, Z., Illingworth, A. J., O'Connor, E. J., Rossow, W. B., Durden, S. L., Miller, S.D., Austin, R. T., Benedetti, A., Mitrescu, C., and the Cloudsat Science Team, *The CloudSat mission and the A-Train: A new dimension of space-based observations of clouds and precipitation*, Bulletin of the American Meteorological Society, Vol. 83, No. 12, 2002, pp. 1771-1790. doi: 10.1175/BAMS-83-12-1771.

[17] Romanazzo, M., Jauregui, L., Morales, J., and Emanuelli, P.P., *Tandem operations preparation for Sentinel-3 A/B: paving the way for C/D models* 2018 SpaceOps Conference, AIAA 2018-2520, 2018. doi: 10.2514/6.2018-2520.

[18] Arnas, D., Casanova, D., and Tresaco, E., *2D Necklace Flower Constellations*, Acta Astronautica, Vol. 142, 2018, pp. 18-28. doi: 10.1016/j.actaastro.2017.10.017.

[19] Arnas, D., Casanova, D., Tresaco, E., and Mortari, D., *3-Dimensional Necklace Flower Constellations*, Celestial Mechanics and Dynamical Astronomy, Vol. 129, No. 4, 2017, pp. 433-448. doi: 10.1007/s10569-017-9789-1.

[20] Arnas, D., Casanova, D., and Tresaco, E., *n-Dimensional congruent lattices using necklaces*, Advances in Space Research, accepted for publication, 2020. doi: 10.1016/j.asr.2020.04.045.

[21] Arnas, D., *Necklace Flower Constellations*, Thesis dissertation, Universidad de Zaragoza, 2018.

[22] Mortari, D., and Wilkins, M. P., *Flower Constellation Set Theory Part I: Compatibility and Phasing*, IEEE Transactions on Aerospace and Electronic Systems, Vol. 44, No. 3, 2008, pp. 953-963. doi: 10.1109/TAES.2008.4655355.

[23] Wilkins, M. P., and Mortari, D., *Flower Constellation Set Theory Part II: Secondary Paths and Equivalency*, IEEE Transactions on Aerospace and Electronic Systems, Vol. 44, No. 3, 2008, pp. 964-976. doi: 10.1109/TAES.2008.4655356.

[24] Avendaño, M. E., and Mortari, D., *New Insights on Flower Constellations Theory*, Journal of IEEE Transactions on Aerospace and Electronic Systems, Vol. 48, No. 2, 2012, pp. 1018-1030. doi: 10.1109/TAES.2012.6178046.

[25] Avendaño, M. E., Davis, J. J. and Mortari, D., *The 2-D Lattice Theory of Flower Constellations*, Celestial Mechanics and Dynamical Astronomy, Vol. 116, No. 4, 2013, pp. 325-337. doi: 10.1007/s10569-013-9493-8.

[26] Davis, J. J., Avendaño, M. E., and Mortari, D., *The 3-D Lattice Theory of Flower Constellations*, Celestial Mechanics and Dynamical Astronomy, Vol. 116, No. 4, 2013, pp. 339-356. doi: 10.1007/s10569-013-9494-7.

[27] Arnas, D., Casanova, D., and Tresaco, E., *4D Lattice Flower Constellations*, Advances in Space Research, accepted for publication, 2020. doi: 10.1016/j.asr.2020.04.018.

[28] Casanova, D., Avendaño, M. E., and Mortari, D., *Design of Flower Constellations using Necklaces*, IEEE Transactions on Aerospace and Electronic Systems, Vol. 50, No. 2, 2014, pp. 1347-1358. doi: 10.1109/TAES.2014.120269.

[29] Lansard, E., Frayssinhes, E.,, and Palmade, J. L., *Global design of satellite constellations: a multi-criteria performance comparison of classical walker patterns and new design patterns*, Acta Astronautica, Vol. 42, No. 9, 1998, pp. 555-564. doi: 10.1016/S0094-5765(98)00043-5.

[30] Han, S., Gui, Q., Li, G., and Du, Y., *Minimum of PDOP and its applications in inter-satellite links (ISL) establishment of Walker-δ constellation*, Advances in Space Research, Vol. 54, No. 4, 2014, pp. 726-733. doi: 10.1016/S0094-5765(98)00043-5.

[31] Lee, S., and Mortari, D., *Design of Constellations for Earth Observation with Intersatellite Links*, AIAA Journal of Guidance, Control and Dynamics, Vol. 40, No. 5, 2017, pp. 1261-1269. doi: 10.2514/1.G001710.

[32] Lee, S., Wu, Y., and Mortari, D., *Satellite constellation design for telecommunication in Antarctica*, International Journal of Satellite Communications and Networking, Vol. 34, No. 6, 2016, pp. 725-737. doi: 10.1002/sat.1128.

[33] Arnas, D., Casanova, D., and Tresaco, E., *Time distributions in satellite constellation design*, Celestial Mechanics and Dynamical Astronomy, Vol. 128, No. 2 - 3, 2017, pp. 197-219. doi: 10.1007/s10569-016-9747-3.

[34] Arnas, D., Casanova, D., and Tresaco, E., *Corrections on repeating ground-track orbits and their applications in satellite constellation design*, Advances in the Astronautical Sciences, Vol. 158, 2016, pp. 2823-2840. ISBN: 978-0-87703-634-0.

[35] Arnas, D., and Casanova, D., *Nominal definition of satellite constellations under the Earth gravitational potential*, Celestial Mechanics and Dynamical Astronomy, Vol. 132, No. 19, 2020. doi: 10.1007/s10569-020-09958-4.

[36] Kéchichian, J. A., *Analysis and implementation of in-plane stationkeeping of continuously perturbed Walker constellations*, Acta Astronautica, Vol. 65, No. 11-12, 2009, pp. 1650-1667. doi: 10.1016/j.actaastro.2009.04.008.

[37] Chao, C.C., *Long-term orbit perturbations of the Draim four-satellite constellations*, Journal of Guidance Control and Dynamics, Vol. 15, No. 6, 2012, pp. 1406-1410. doi: 10.2514/3.11403.

[38] Bruno, M.J., and Pernicka, H.J., *Tundra Constellation Design and Stationkeeping*, Journal of Spacecraft and Rockets, Vol. 42, No. 5, 2005, pp. 902-912 . doi: 10.2514/1.7765.

[39] Deleflie, F., Legendre, P., Exertier, P., and Barlier, F., *Long term evolution of the Galileo constellation due to gravitational forces*, Advances in Space Research, Vol. 36, No. 3, 2005, pp. 402-411. doi: 10.1016/j.asr.2005.04.056.

[40] Mortari, D., Avendaño, M. E. and Lee, S., *J2-Propelled Orbits and Constellations*, Journal of Guidance, Control, and Dynamics, Vol. 37, No. 5, 2014, pp. 1701-1706. doi: 10.2514/1.G000363.

[41] Arnas, D., Casanova, D., and Tresaco, E., *Relative and absolute station-keeping for two-dimensional-lattice flower constellations*, Journal of

Guidance, Control, and Dynamics, Vol. 39, No. 11, 2016, pp. 2596-2602. doi: 10.2514/1.G000358.

[42] Arnas, D., Jurado, P., Barat, I., Dusmann, B., and Bock, R, *FLEX: a parametric study of its tandem formation with Sentinel-3* IEEE Journal of Selected Topics in Applied Earth Observations and Remote Sensing, Vol. 12, No. 7, 2019, pp. 2447-2452. doi: 10.1109/JSTARS.2019.2896196.

[43] Lee, D. S., Storey, J. C., Choate, M. J., and Hayes, R. W., *Four years of Landsat-7 on-orbit geometric calibration and performance*, IEEE Transactions on Geoscience and Remote Sensing, Vol. 42, No. 12, 2004, pp. 2786-2795. doi: 10.1109/TGRS.2004.836769.

[44] Hammerling, D. M., Michalak, A. M., and Kawa, S. R., *Mapping of CO2 at high spatiotemporal resolution using satellite observations: Global distributions from OCO-2*, Journal of Geophysical Research: Atmospheres, Vol. 117, D06306, 2012. doi: 10.1029/2011JD017015.

[45] Chander, G., Markham, B. L., and Helder, D. L., *Summary of current radiometric calibration coefficients for Landsat MSS, TM, ETM+, and EO-1 ALI sensors*, Remote sensing of environment, Vol. 113, No. 5, 2009, pp. 893-903. doi: 10.1016/j.rse.2009.01.007.

[46] Teillet, P. M., Barker, J. L., Markham, B. L., Irish, R. R., Fedosejevs, G., and Storey, J. C., *Radiometric cross-calibration of the Landsat-7 ETM+ and Landsat-5 TM sensors based on tandem data sets*, Remote sensing of environment, Vol. 78, No. 1, 2001, pp. 39-54. doi: 10.1016/S0034-4257(01)00248-6.

[47] Chander, G., Meyer, D. J., and Helder, D. L., *Cross calibration of the Landsat-7 ETM+ and EO-1 ALI sensor*, IEEE Transactions on Geoscience and Remote Sensing, Vol. 42, No. 12, 2004, pp. 2821-2831. doi: 10.1109/TGRS.2004.836387.

[48] Parkinson, C. L., Ward, A., and King, M. D., *Earth science reference handbook: a guide to NASA's earth science program and earth observing satellite missions*, National Aeronautics and Space Administration, 277, 2006.

[49] Vallado, D.: *Fundamentals of Astrodynamics and Applications*, Microcosm Press, 2013. ISBN: 978-1881883197.

[50] Liu, J. J. F., and Alford, R. L., *Semianalytic theory for a close-Earth artificial satellite*, Journal of Guidance, Control, and Dynamics, Vol. 3, No. 4, 1980, pp. 304-311. doi: 10.2514/3.55994.

[51] Kozai, Y., *Second-order solution of artificial satellite theory without air drag*, The Astronomical Journal, Vol. 67, 1962, pp. 446-461.

[52] Liu, J. J. F., *Satellite Motion about an Oblate Earth*, AIAA Journal, Vol. 12, No. 11, 1974, pp. 1511-1516. doi: 10.2514/3.49537.

[53] Wagner, C., *A Prograde Geosat Exact Repeat Mission?*, Journal of the Astronautical Sciences, Vol. 39, 1991, pp. 313-326.

[54] Picone, J.M., Hedin, A.E., Drob. D.P., and Aikin, A.C., *NRLMSISE-00 empirical model of the atmosphere: statistical comparisons and scientific issues*, Journal of Geophysical Research: Space Physics, Vol. 107, No. A12, 2002, pp. SIA-15. doi: 10.1029/2002JA009430.

[55] European Cooperation for Space Standardization (ECSS) *Space Engineering: Space Environment, standard ECSS-E-10-04A*, ESA publications, Jan 2000.

[56] Arnas, D., Lifson, M., Linares, R., and Avendaño, M.E., *Definition of Low Earth Orbit Slotting Architectures Using 2D Lattice Flower Constellations*, Advances in Space Research, accepted for publication, 2020. doi: 10.1016/j.asr.2020.04.021.